Relaxation processes of the Ge-H stretch modes in hydrogenated amorphous germanium

K. W. Jobson,[1] J.-P. R. Wells,[1,*] R. E. I. Schropp,[2] D. A. Carder,[3] P. J. Phillips,[3] and J. I. Dijkhuis[2]
[1]*Department of Physics and Astronomy, University of Sheffield, Sheffield S3 7RH, United Kingdom*
[2]*Debye Institute, University of Utrecht, P.O. Box 80000, TA 3508 Utrecht, The Netherlands*
[3]*FELIX Free Electron Laser Facility, FOM-Institute for Plasmaphysics "Rijnhuizen," P.O. Box 1207, 3430 BE Nieuwegein, The Netherlands*
(Received 4 October 2005; revised manuscript received 12 December 2005; published 3 April 2006)

Infrared transient grating measurements on the Ge-H stretch mode at 1880 cm^{-1} in hydrogenated amorphous germanium show a long, multiexponential relaxation time having a mean decay constant of 306 ps. The thermal activation of the decay rate suggests a decay via two Ge-H bending modes with the energy mismatch bridged by three bulk Ge-Ge vibrations. From the probe pulse diffraction efficiency, we have determined a value for the nonlinear refractive index of $n_2=5.9\times10^{-4}$ cm^2/GW. Utilizing the photon echo technique, we determine that the dominant contribution to a vibrational dephasing near room temperature is the elastic scattering of TO modes near 270 cm^{-1}. At 10 K additional dephasing from nonequilibrium phonons are readily observable as an excitation dependent contribution.

DOI: 10.1103/PhysRevB.73.155202 PACS number(s): 39.30.+w, 78.47.+p, 82.53.Kp, 63.20.Pw

I. INTRODUCTION

Hydrogenated amorphous silicon (*a*-Si:H) has been widely studied. It is appealing due to its low cost and has found many applications in large area optoelectronics technology, in particular, solar cells. By alloying (*a*-Si:H) with germanium, it is possible to reduce the band gap and thereby improve the long wavelength response. As increasing quantities of germanium are added, however, there is a sharp deterioration of the photoconductive response which can be as high as several orders of magnitude.[1] Plasma enhanced chemical vapor deposition (PECVD) is the technique of choice for device quality layers and it is notable that a-Ge:H prepared under similar conditions to (*a*-Si:H) shows a larger deep gap state density.[2,3] Later work has shown that better quality films of (*a*-SiGe:H), films that exhibit lower densities of deep gap states and a lack of microstructure, can be grown under low pressure, high ion flux conditions.[4] In fact, significantly fewer studies report measurements of hydrogenated amorphous germanium (*a*-Ge:H), though it has been shown that the best device quality films have been obtained for growth in the presence of an excess of hydrogen.[5] An additional and important issue is that the Staebler-Wronski effect (light induced degradation due to defect creation), a significant and perennial factor in *a*-Si:H and the exact dynamics of which are still unclear, is observed in *a*-Ge:H (Ref. 6) and in *a*-SiGe:H for germanium rich alloys.[7]

We report on infrared, degenerate four wave mixing experiments performed resonant with the Ge-H stretch mode in hydrogenated amorphous germanium thin films. Important earlier work in this context includes infrared absorption and Raman spectroscopy of *a*-Ge, *a*-Ge:H thin films, and *a*-Ge/SiO_x superlattices.[8,9] The dominant infrared features associated with growth in germane gas are the Ge-H bond stretching and bending vibrational modes at 1880 and 560 cm^{-1}, respectively,[10,11] for *a*-Ge:H thin films. No previous time resolved measurements have been performed for localized modes in *a*-Ge, despite the wealth of time-resolved experiments performed on the localized modes of various different forms of silicon (an overview of which can be found in Ref. 12), including the dynamics of both hydrogenated and deuterated amorphous silicon.[13–15] These experiments revealed several important aspects of vibrational relaxation in amorphous silicon, these being that the Si-H stretch mode does not form a phononlike band of states, being instead a highly localized vibration and that the local environment of the Si-H bond strongly influences the relaxation time.

II. EXPERIMENT

The samples consisted of a 2.1 μm thick *a*-Ge layer deposited using PECVD at 13.56 MHz, on a 250 μm *c*-Si substrate which is transparent at the infrared wavelengths of interest in this work. All samples were assessed using linear infrared absorption with a dry N_2 purged Nicolet Fourier transform infrared spectrometer. The nonlinear infrared measurements were performed using the Dutch free electron laser FELIX which is situated in Nieuwegein, and is continuously tunable from 250–4.3 μm and therefore over the 6.5–5 μm region of interest.

In both the transient grating and photon echo experiments, FELIX was resonant with the $\nu=0\rightarrow1$ fundamental transition of the Ge-H stretch mode at a wavelength close to 5.32 μm. The output of FELIX is a macropulse of ~4 μs having a repetition rate of either 5 or 10 Hz. Each macropulse consists of 100 micropulses having a repetition rate of 25 MHz. The micropulses are variable in length between 500 and 5 ps. The transient grating measurements were performed in the "forward box" geometry, with two noncolinear pump beams (having wave vectors $\mathbf{k}_1$ and $\mathbf{k}_2$) spatially and temporally overlapped on the sample creating a vibrational population grating. A weaker, spatially overlapped but time delayed probe beam (with wave vector $\mathbf{k}_3$) is then Bragg diffracted off this grating into a phase matched signal direction ($\mathbf{k}_4=\mathbf{k}_1-\mathbf{k}_2+\mathbf{k}_3$), with a signal intensity that decays as $T_1/2$ for variable delays between the fixed pump pulses and the probe. From the angle θ_p, of 13° between the pump

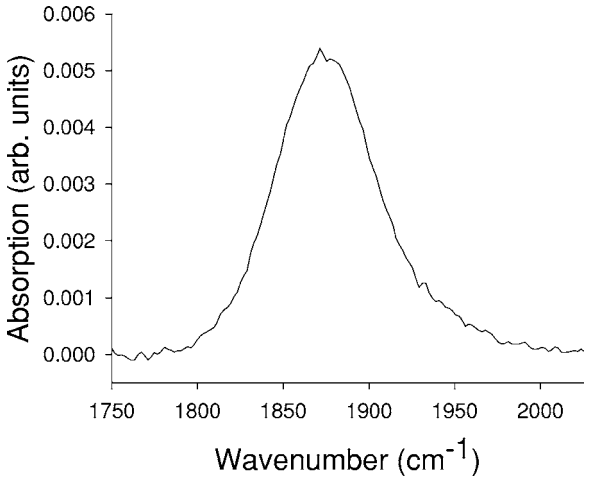

FIG. 1. Infrared absorption spectrum of *a*-Ge:H.

beams we deduce a grating period $[\lambda_p/2\sin(\theta_p/2)$ with λ_p the pump wavelength] of 23.5 μm. The maximum grating efficiency $\eta(\tau)$ that could be observed at zero delay between the pump and probe pulses was 2.35×10^{-3} for a total pump irradiance of 66.2 GW/cm^2. Since the scattering efficiency for an optically thin refractive index grating is $\eta(\tau) \cong [k\Delta n(\tau)d/2]^2$ where k is the probe wave vector and d is the sample thickness, we can, therefore, infer a refractive index change $\Delta n(0)=0.0391$. Relating this change to an effective nonlinear refractive coefficient n_2 [through $\Delta n(0) = n_2 I_0$, where I_0 is the pump beam irradiance] we obtain an n_2 value 5.9×10^{-4} cm^2/GW. The photon echo measurement relies upon a two pulse sequence that is applied to the sample such that the first pulse (having wave vector $\mathbf{k}_1$) creates a coherent superposition of vibrational states. Immediately after the first pulse all of the microscopic dipoles oscillate in phase. Due to the distribution of frequencies within the inhomogeneous line shape, this initial phase relation is rapidly lost. At a time τ later a second pulse (with wave vector $\mathbf{k}_2$) causes an inversion of the macroscopic dipole moment which leads to a rephasing of these individual frequency components, yielding at an additional time τ, a phase matched superradiant burst from the rephrased ensemble which is known as a photon echo. The time integrated echo signal propagating along the $\mathbf{k}_{\text{echo}}=|2\mathbf{k}_2-\mathbf{k}_1|$ signal direction decays as a function of the delay between the incoming pulses as $T_2/4$. Both the diffracted probe of the transient grating measurement and the echo signal are "background free" measurements allowing for excellent signal to noise ratios, which we measure on a liquid nitrogen cooled mercury cadmium telluride detector with the signal averaging provided using boxcar integration.

III. RESULTS

Figure 1 shows the room temperature infrared absorption spectrum of *a*-Ge:H. The sample contains around 3.5 at. % H and the absorption peak near 1880 cm^{-1} (5.32 μm) is attributable to the fundamental frequency of the stretching vibration of isolated Ge-H bonds. The linewidth

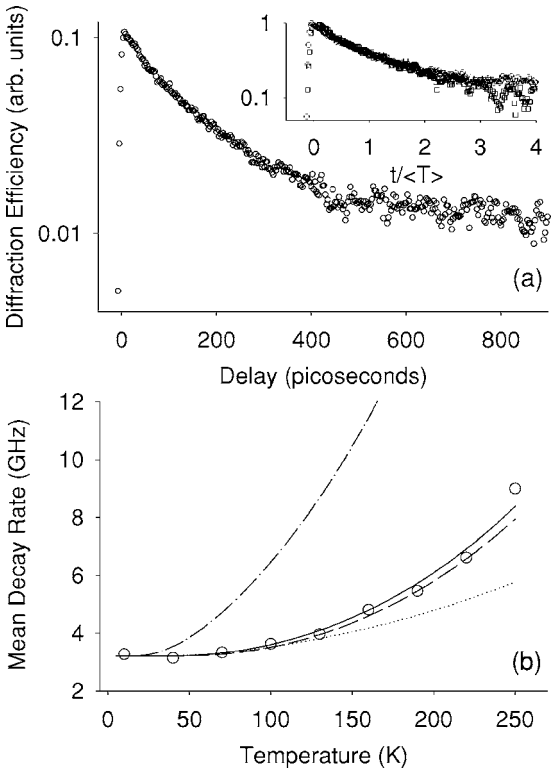

FIG. 2. (a) 10 K transient grating signals for resonant excitation of the Ge-H stretch modes at 5.32 μm Inset: The superimposed transient grating signals at 10 K (open circles) and 220 K (open squares), (b) the temperature dependent, mean vibrational population decay rates. The dotted line is the decay into 3 Ge-H bending modes at 560 cm^{-1} and 1 LA mode at 170 cm^{-1}; the dashed-dotted line is the decay into 3 Ge-H bending modes and 2 TA modes at 85 cm^{-1}; the dashed line is the decay into 2 bending modes and 3 LO modes at 247 cm^{-1}, while the solid line shows the decay into 2 bending modes, two TO modes at 280 cm^{-1}, and 1 LA mode at 180 cm^{-1}.

of the $\nu=0\rightarrow1$ transition exceeds 60 cm^{-1} at all temperatures and therefore the line broadening is dominated by variations in the Ge-H bond angles due to the amorphous environment. It is noticeable in the data that there is a slight asymmetry on the blue side of the absorption peak that could be attributable to additional absorbing species. This is certainly not due to absorption from polyhydride bonding configurations (Ge-H$_x$) as the peak of these modes is found at 2000 cm^{-1}.[10,16,17] We also note that it is unlikely that this extra absorption could contribute to the measured degenerate four wave mixing (DFWM) signals as the bandwidth of the FELIX beam was set to $\sim$36 cm^{-1} in all experiments, thus putting the asymmetric feature beyond the range of the power spectrum of the FELIX pulse.

A. Vibrational lifetime measurements

Figure 2(a) shows the 10 K laser induced transient grating signal for a resonant excitation of the *a*-Ge:H stretch mode near the absorption peak at 5.32 μm. The characteristic feature of the transients at all temperatures is their nonexponential decay. Notably, similar effects were observed for the vi-

brational relaxation of Si-H stretch modes in *a*-Si:H (Ref. 14) but are not observed either in the crystalline silicon counterpart nor for Si-D stretch modes in *a*-Si:D.[15] Following Ref. 14, we have determined that the temporally normalized transient grating traces at any temperature or excitation density, can be merged on to a single curve [see inset to Fig. 2(a)] by rescaling the time axis of each curve $S_g(t)$ with the average time $\langle T_g\rangle = \int t S_g(t)dt / \int S_g(t)dt$ of that curve. Using the ratios between the average times at different temperatures, the temperature dependence of the mean decay rate is determined. The absolute value of the mean decay time for the 10 K transient is $\langle T_1(10\ \mathrm{K})\rangle = 306$ ps. An additional feature of the transient gratings signals is a long time decay representing up to 10% of the signal amplitude and not decaying on the scale of the measurement (~900 ps).

The anharmonic break of a vibrational mode having frequency ω into any combination of accepting vibrations with frequencies ω_i proceeds with a temperature dependent decay rate $[T_1(T)]^{-1}$ that can be described by[18]

$$[T_1(T)]^{-1} = [T_1(0)]^{-1}\left(\frac{\exp(\hbar\omega/k_BT)-1}{\Pi_i[\exp(\hbar\omega_i/k_BT)-1]}\right), \qquad (1)$$

where $[T_1(0)]^{-1}$ is the zero temperature decay rate and $\Sigma_i \hbar\omega_i = \hbar\omega$ in order to satisfy energy conservation. Figure 2(b) shows the temperature dependent mean decay rate with the experimental data shown as open circles. We approximate $[T_1(0)]^{-1}$ by the 10 K value of 3.21 GHz. The dotted line shows the predicted decay rate for relaxation into four accepting modes: three Ge-H bending modes at 560 cm^{-1} and a single longitudinal acoustic (LA) mode at 170 cm^{-1} to bridge the energy mismatch. As can be seen in Fig. 2(b), this significantly underestimates the increase of the decay rate with increasing temperature. The dashed-dotted line represents decay into five accepting modes: three Ge-H bending modes and two low frequency transverse acoustic (TA) modes at 85 cm^{-1}. This approximation radically overestimates the decay rate at all temperatures above 30 K due to the low activation energies associated with the TA modes. The most accurate account of the data can be obtained for decay into either two bending modes and three longitudinal optical (LO) modes at 247 cm^{-1} (shown as a dashed line) or two bending modes, two transverse optical (TO) modes at 280 cm^{-1} and a single LA mode at 180 cm^{-1} (shown as a solid line). Given the experimental uncertainties, it would not be realistic to attempt to discriminate between the two possibilities. However, regardless of the exact decay pathway, it is certainly true that the stretching mode decays via two bending modes, with the excess energy then bridged by the Ge-Ge vibrations, in this case being either three LO modes or two TO and one LA mode. What does seem clear is that the origin of the nonexponential decay is associated with decay into Ge-H bending vibrations in the amorphous host. Both these points have already been shown to occur in the case of amorphous silicon and are discussed fully in Ref. 14.

B. Photon echo spectroscopy

Figure 3(a) shows a representative photon echo trace measured at 10 K. From the mean homogeneous dephasing time $\langle T_2(10\ \mathrm{K})\rangle$ of 158 ps, we infer an equivalent mean homogeneous linewidth $1/\pi\langle T_2\rangle$ of 0.067 cm^{-1} confirming the (reasonable) assertion made earlier that the linewidth is massively inhomogeneously broadened. In order to examine the pure dephasing times T_2^*, the transient grating and photon echo signals [$S_g(t)$ and $S_p(t)$, respectively] must be combined in a similar fashion to Ref. 14. Here $S_g(t)$ and $S_p(t)$ are assumed to be produced from an ensemble of oscillators that has a distribution of population relaxation and dephasing times, $g_1(T_1)$, and $g_2(T_2)$, respectively. This assumption is supported by our observation of nonexponential decay. Then the distribution of dephasing times is broken down into two contributions: one from the population relaxation and the other from the pure dephasing so that $g_2(T_2)dT_2 = g_1(T_1)dT_1 g(T_2^*)dT_2^*$. By normalizing the decay of the echo signal to the decay of the grating signal and then taking the ratio $S_p(t)/S_g(t)$, the lifetime component of the decay is eliminated, $S_p(t)/S_g(t) \propto \int g(T_2^*)e^{-4t/T_2^*}dT_2^*$, leaving only the desired contribution from the pure dephasing. Figure 3(b) shows the ratio $S_p(t)/S_g(t)$ at a representative temperature of

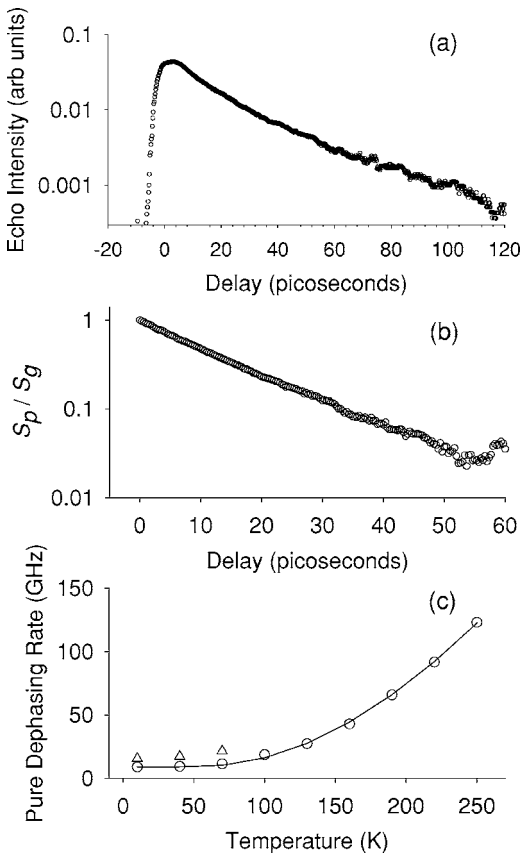

FIG. 3. (a) 10 K photon echo signal for resonant excitation of the Ge-H stretch modes at 5.32 μm, (b) the $S_p(t)/S_g(t)$ ratio at 100 K illustrating single exponential pure dephasing, and (c) the temperature dependence of the pure dephasing rate. The data shown as open triangles are recorded at three times the excitation density of the data shown as open circles. The solid line is a fit to Eq. (2) with $a = 9.0$ GHz and $A = 336$ GHz with elastic scattering from a single vibrational mode having an energy of 270 cm^{-1}.

100 K, which illustrates that the pure dephasing is a single exponential as is found in hydrogenated amorphous silicon. Thus the nonexponentially of the low temperature photon echo traces reflect the significance of the contribution from population decay to the homogeneous dephasing at those temperatures. At high temperatures both the pure dephasing and homogeneous dephasing are essentially single exponential. The temperature dependence of the pure dephasing is shown in Fig. 3(c). As with previous studies on *a*-Si:H/D (Refs. 14 and 15) stretch modes the measured homogeneous dephasing rate is not strictly limited by the population decay at 10 K. This excess dephasing has been attributed to residual long-lived (i.e., exceeding the 40-ns repetition rate of the micropulses of the free electron laser (FEL) nonequilibrium phonons created in the anharmonic break up of the initially excited stretch modes; in other words, the decay products created by the preceding FELIX micropulse. Thus we suggest that the Ge-Ge vibrations in *a*-Ge have similar long lifetimes (i.e., greater than 40 ns) to those measured by time-resolved Raman spectroscopy[19] in *a*-Si. The open triangles and circles in Fig. 3(b) represent echo measurements performed with excitation densities differing by a factor of 3 with the higher excitation density corresponding to the larger pure dephasing rate (consistent with the proposed explanation). The solid line is a fit to

$$[T_2^*(T)]^{-1} = a + An_\omega(n_{\omega'} + 1) \tag{2}$$

which describes elastic phonon scattering of a single Ge-Ge vibrational mode with a being a constant to account for residual dephasing due to nonequilibrium phonons, A is a coupling constant, and $n\omega$ the Bose-Einstein occupancy factor. Through least squares fitting of Eq. (2) to the temperature dependent pure dephasing data, we obtain parameters of $a=9.0$ GHz, $A=336$ GHz with elastic scattering of TO modes near 270 cm^{-1}.[8]

C. Single micropulse experiments

In order to further investigate the influence of the FELIX macropulse on the dephasing signals, we have also performed our measurements using a single micropulse extracted from the macropulse using a pulse slicer. The discrimination of the slicer against all micropulses other than the selected pulse was better than 30:1. The measured 10 K signal (shown in Fig. 4) yields a homogeneous dephasing time of $T_2=385$ ps, considerably longer than the experiments using the entire macropulse and consistent with our explanation. It is important to note that this corresponds to a pure dephasing rate of ~1 GHz, which, within experimental error, falls on the line of Eq. (2) with $a=0$. Regrettably, since FELIX operates at 5 Hz the signal averaging capability using the pulse slicer is limited and attempts to perform detailed power dependencies were not reliable. However, the current data indicate that the single micropulse data is power dependent, though significantly less so than experiments performed with the full FELIX macropulse. Other explanations for the observed power dependence such as excitation induced dephasing are unlikely given the low hydrogen content (3.5 at. %) present in the sample, while simple explanations such as heating under the full macropulse fluence cannot account for the increase in the dephasing rates. Furthermore, recording the dephasing times either within the first 500 ns or the last 500 ns of the macropulse (by changing the temporal position of the gate of the boxcar integrator) does not noticeably alter the results.

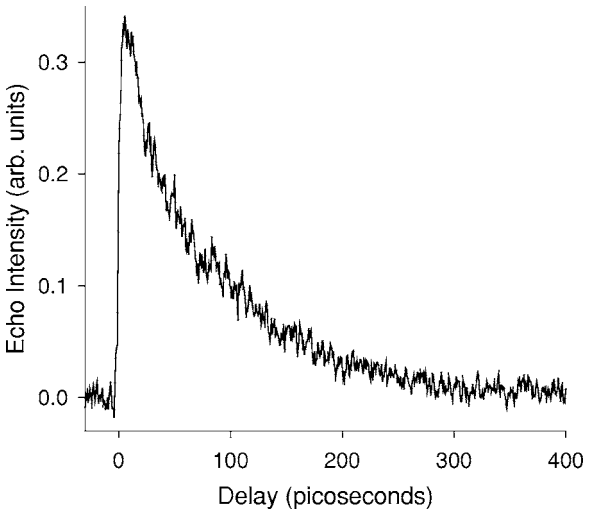

FIG. 4. 10 K photon echo signal using a single FELIX micropulse per macropulse.

IV. CONCLUSIONS

We report on degenerate four wave mixing measurements of vibrational population and phase relaxation of Ge-H stretching modes in *a*-Ge:H using the Dutch free electron laser, FELIX. Infrared transient grating measurements reveal multiexponential population decay due to the amorphous surroundings of the host material. From the temperature dependence of the observed decay rates, we infer that the Ge-H stretch modes decay into two bending vibrations with the energy mismatch absorbed by Ge-Ge vibrations. Photon echo experiments reveal both an excitation and temperature dependent contributions to the vibrational dephasing. The temperature dependent contribution is governed by elastic scatterings of Ge-Ge vibrations which seem to be dominated by TO modes near 270 cm^{-1}. We ascribe the excitation dependence to additional dephasing contributions from nonequilibrium phonons created in the anharmonic decay of Ge-H stretch vibrations excited by the preceding micropulse of the FELIX macropulse. Using a pulse slicer to extract a single FELIX micropulse, we observe a homogeneous dephasing time a factor of nearly 2.4 longer for the same pulse energies, consistent with our model.

ACKNOWLEDGMENTS

We gratefully acknowledge the support by the *Stichting voor Fundamenteel Onderzoek der Materie* (FOM) in providing the required beamtime on FELIX and would like to thank the FELIX staff for their assistance. We would also like to thank Karine van der Werf for preparing the a-Ge:H layers on double polished substrates at short notice.

*Corresponding author. FAX: +44-(0)114-2728079. Email address: j.p.wells@sheffield.ac.uk

[1] Y.-P. Chou and S.-C. Lee, J. Appl. Phys. **83**, 4111 (1998).
[2] A. Skumanich and N. M. Amer, J. Non-Cryst. Solids **59-60**, 249 (1983).
[3] Y. Bouizem, A. Belfedal, J. D. Sib, A. Kebab, and L. Chahed, J. Phys.: Condens. Matter **17**, 5149 (2005).
[4] V. L. Dalal, Y. Liu, Z. Zhou, and K. Han, J. Non-Cryst. Solids **299-302**, 1127 (2002).
[5] J. Zhu, V. L. Dalal, M. A. Ring, J. J. Gutierrez, and J. D. Cohen, J. Non-Cryst. Solids **338-340**, 651 (2004).
[6] J. Whitaker, M. M. de Lima, F. C. Marques, and P. C. Taylor, J. Non-Cryst. Solids **338-340**, 374 (2004).
[7] V. Chu, J. P. Conde, S. Aljishi, and S. Wagner, Mater. Res. Soc. Symp. Proc. **118**, 167 (1988).
[8] S. C. Shen, C. J. Fang, M. Cardona, and L. Genzel, Phys. Rev. B **22**, 2913 (1980).
[9] G. V. M. Williams, A. Bittar, and H. J. Trodahl, J. Appl. Phys. **64**, 5148 (1988).
[10] M. K. Bhan, L. K. Malhotra, and S. C. Kashyap, J. Appl. Phys. **65**, 241 (1988).
[11] C. Godet, I. El Zawawi, M. L. Thèye, M. Gauthier, and J. P. Stoquert, Solid State Commun. **74**, 721 (1990).
[12] G. Lüpke, N. H. Tolk, and L. C. Feldman, J. Appl. Phys. **93**, 2317 (2003).
[13] Z. Xu, P. M. Fauchet, C. W. Rella, H. A. Schwettman, and C. C. Tsai, J. Non-Cryst. Solids **198-200**, 11 (1996).
[14] M. van der Voort, C. W. Rella, L. F. G. van der Meer, A. V. Akimov, and J. I. Dijkhuis, Phys. Rev. Lett. **84**, 1236 (2000).
[15] J. P. R. Wells, R. E. I. Schropp, L. F. G. van der Meer, and J. I. Dijkhuis, Phys. Rev. Lett. **89**, 125504 (2002).
[16] G. Lucovsky, S. S. Chao, J. Yang, J. E. Tyler, R. C. Ross, and W. Czubatyj, Phys. Rev. B **31**, 2190 (1985).
[17] D. Bermejo and M. Cardona, J. Non-Cryst. Solids **32**, 421 (1979).
[18] A. Nitzan, S. Mukamel, and J. Jortner, J. Chem. Phys. **60**, 3929 (1974).
[19] M. van der Voort, O. L. Muskens, A. V. Akimov, A. B. Pevtsov, and J. I. Dijkhuis, Phys. Rev. B **64**, 045203 (2001).